FULL PAPER



Check for updates

Absolute configuration of cytotoxic anthraquinones from a Brazilian cave soil-derived fungus, *Aspergillus* sp. SDC28

Juliana R. Gubiani¹ | Darlon I. Bernardi¹ | Caio C. P. De Paula^{2,3} | Mirna H. R. Seleghim² | Antonio G. Ferreira⁴ | Andrea N. L. Batista⁵ | João M. Batista Jr.⁶ | Lucianne F. P. Oliveira⁷ | Simone P. Lira⁷ | Joanna E. Burdette⁸ | Roberto G. S. Berlinck¹ |

Correspondence

João M. Batista Jr., Instituto de Ciência e Tecnologia, Universidade Federal de São Paulo, São José dos Campos, Brazil. Email: batista.junior@unifesp.br

Roberto G. S. Berlinck, Instituto de Química de São Carlos, Universidade de São Paulo, CP 780, CEP 13560-970 São Carlos, SP, Brazil. Email: rgsberlinck@iqsc.usp.br

Funding information

National Institutes of Health, Grant/Award Number: P01CA125066; Fundação de Amparo à Pesquisa do Estado de São Paulo, Grant/Award Numbers: 2013/ 50228-8, 2016/21341-9, 2017/06014-4, 2017/12436-9, 2019/22319-5, 2019/ 17721-9

Abstract

Microbial strains isolated from extreme and understudied environments, such as caves, are still poorly investigated for the production of bioactive secondary metabolites. Investigation of the ethyl acetate extract from the growth medium produced by the soil-derived fungus Aspergillus sp. SDC28, isolated from a Brazilian cave, yielded two anthraquinones: versicolorin C (1) and versiconol (2). The complete assignment of nuclear magnetic resonance and mass spectroscopic data of 1 and 2 was performed for the first time. Moreover, the yet unreported absolute configuration of both compounds was unambiguously established by analysis of experimental and theoretical electronic circular dichroism data. Vibrational circular dichroism was also applied to confirm the absolute stereochemistry of 2. Compounds 1 and 2 showed cytotoxic activity against human ovarian cancer cells (OVCAR3).

KEYWORDS

anticancer, aromatic metabolites, extremophiles, polyketides, soil-derived fungus

Abbreviations: COSY, correlation spectroscopy; DFT, density functional theory; DMSO, dimethylsulfoxide; ECD, electronic circular dichroism; HMBC, heteronuclear multiple bond correlation; HRESITOFMS, high-resolution electrospray ionization time of flight mass spectrum; HSQC, heteronuclear single quantum coherence; IR, infrared; NMR, nuclear magnetic resonance; NOESY, nuclear overhauser effect spectroscopy; OVCAR3, human ovarian cancer cell line; VCD, vibrational circular dichroism.

© 2022 Deutsche Pharmazeutische Gesellschaft

¹Instituto de Química de São Carlos, Universidade de São Paulo, São Carlos, Brazil

²Departamento de Ecologia e Biologia Evolutiva, Universidade Federal de São Carlos, São Carlos, Brazil

³Biology Centre CAS, Institute of Hydrobiology, České Budějovice, Czech Republic

⁴Departamento de Química, Universidade Federal de São Carlos, São Carlos, Brazil

⁵Instituto de Química, Universidade Federal Fluminense, Niterói, Brazil

⁶Instituto de Ciência e Tecnologia, Universidade Federal de São Paulo, São José dos Campos, Brazil

⁷Departamento de Ciências Exatas, Escola Superior de Agricultura Luiz de Queiroz, Universidade de São Paulo, Piracicaba, Brazil

⁸Pharmaceutical Sciences, College of Pharmacy, University of Illinois, Ashland, Oregon, USA

Caves are subterranean extreme environments considered as oligotrophic, in permanent darkness, high humidity, and constant temperature, with a tendency toward environmental constancy in the deep zone, providing highly specialized habitat niches. Nevertheless, caves have been overlooked, considering its potential for the discovery of new genetic resources. [1-4] Subterranean ecosystems usually have a distinctive biota, in which microbes play an important ecological role. Microscopic fungi are relevant components of caves' microflora, being found in sediments, vermiculations, bat droppings, and/or guano and decaying organic material. [4,5]

Caves harbor a diverse array of parasitic and decomposing fungi. More than 1150 fungi species have been discovered and identified from caves. Caves' pathogenic fungi received more attention due to health and economic concerns. Caves' fungi are also saprophytic organisms, with a complex biochemical machinery to produce and release the secondary metabolites.^[6]

Previous investigations of caves' fungi are related to taxonomy or geomicrobiology, damages on rock-art paintings, or the caves' colonization by fungi.^[7,8] A study at the Chaabe Cave in Algeria demonstrated that among the 23 strains of fungi isolated at that specific location, 73% showed significant inhibitory activity against pathogenic microorganisms.^[9] A microbiological investigation on fungi from Lapa Nova Cave (Minas Gerais state, Brazil) described the isolation of 2,575 strains, the more diverse genera being Aspergillus, Calcarisporium, Chaetomium, Cladosporium, Curvularia, Emericella, Eurotium, Fusarium, Geotrichum, Gliocladium, Mucor, Purpureocillium, Paecilomyces, Penicillium, Rhizopus, and Trichoderma.^[4] Several strains isolated during the above-mentioned investigation showed resistance to the antifungal amphotericin B. itraconazole, voriconazole, and terbinafine.[10] A subsequent investigation on fungi from a Brazilian cave showed that, among eight fungal isolates selected based on their pigment production in solid culture media, only one (Penicillium flavigenum CML2965) showed antioxidant activity, assigned to gallic acid, catechin, chlorogenic acid, caffeic acid, and vanillin.^[11] Pigments were identified to be produced by three fungi from Brazilian caves, Aspergillus keveii, P. flavigenum, and Epicoccum nigrum.[12] Although the secondary metabolism of Aspergillus spp. strains has been extensively investigated, [13] new bioactive secondary metabolites continue to be isolated from cultures of Aspergillus spp. strains.[14-16]

Herein, we describe the investigation of cultures produced by Aspergillus sp. SDC28 isolated from Catão cave (São Desidério karst area, Bahia state, Brazil), from which versicolorin C (1) and versiconol (2) (Figure 1) have been isolated and identified. We assigned the complete spectroscopic data for both 1 and 2 for the first time. Moreover, versicolorin C (1) had its absolute configuration established for the first time by analysis of electronic circular dichroism (ECD) data. The absolute configuration of versiconol (2) was assigned using a combination of ECD and vibrational circular dichroism (VCD) methods. Both compounds showed cytotoxic activity against ovarian cancer cells OVCAR3.

2 | RESULTS AND DISCUSSION

2.1 | Chemistry

Versicolorin C (1) was isolated as an orange amorphous powder. It showed an [M-H] ion in its HRESITOFMS at m/z 339.0506, corresponding to the formula C₁₈H₁₂O₇, with 13 degrees of unsaturation (DI). Analysis of the ¹H, ¹³C (Table 1), and HSQC nuclear magnetic resonance (NMR) spectra of 1 showed two sp3 methylene groups at δ_H 4.10/3.50 (t, J = 8.2 Hz, m; δ_C 67.4, CH_2 -3′) and δ_H 2.18 (m; δ_C 30.4, CH_2 -4') as well as two sp^3 methine groups at δ_H 4.16 (t, J = 7.0 Hz; δ_C 43.7, CH-2′) and δ_H 6.54 (d, J = 5.7 Hz; δ_C 113.5, CH-1'). Signals of three sp^2 methine hydrogens were observed at δ_H 6.60 (d, J = 2.4 Hz; δ_C 109.1, CH-7), δ_H 7.13 (d, J = 2.34 Hz; δ_C 108.7, CH-5), and δ_{H} 7.09 (s; δ_{C} 101.6, CH-4), along with two carbonyl carbons at δ_C 181.2 (C-10) and δ_C 189.4 (C-9) as well as sp^2 quaternary carbons δ_C 159.2 (C-1), δ_C 120.4 (C-2), δ_C 165.6 (C-3), $\delta_{\rm C}$ 135.7 (C-4a), $\delta_{\rm C}$ 165.5 (C-6), $\delta_{\rm C}$ 164.5 (C-8), $\delta_{\rm C}$ 108.3 (C-8a), $\delta_{\rm C}$ 111.1 (C-9a), and δ_C 135.1 (C-10a). Analysis of the ¹H and ¹³C NMR spectra of 1 indicated an anthraquinone skeleton.

A 1,3,4,5-tetrasubstituted benzene moiety was present in 1 based on the hydrogen signals at $\delta_{\rm H}$ 6.60 (d, J = 2.4 Hz; $\delta_{\rm C}$ 109.1, CH-7) and $\delta_{\rm H}$ 7.13 (d, J = 2.34 Hz; $\delta_{\rm C}$ 108.7, CH-5). The HMBC spectrum showed correlations between H-5 and C-8a, C-10 and C-10a, and H-7 and C-8a (Figure 2), indicating the connection between the 1,3,4,5-substituted benzene moiety and the quinone moiety.

An additional 1,2,3,4,5-pentasubstituted benzene moiety was identified and based on HMBC cross-peaks observed between H-4 and C-2 ($\delta_{\rm C}$ 120.4), C-3 ($\delta_{\rm C}$ 165.6), C-4a ($\delta_{\rm C}$ 135.7), C-9a ($\delta_{\rm C}$ 111.1), and C-10 ($\delta_{\rm C}$ 181.2). Based on these correlations, it was possible to

FIGURE 1 Structures of versicolorin C (1) and versiconol (2)

TABLE 1 ¹H (600 MHz) and ¹³C (150 MHz) NMR spectroscopic data of 1 and 2 in DMSO-d₆

Position	1			2		
	$\delta_{\rm C}$, type	δ _H (J in Hz)	HMBC correlations	δ_{C} , type	δ _H (J in Hz)	HMBC correlations
1	159.2, C			163.2, C		
2	120.4, C			123.0, C		
3	165.6, C			163.6, C		
4	101.6, CH	7.09 (s)	C-2, C-3, C-4a, C-9a, C-10	108.7, CH	7.18 (s)	C-2, C-3, C-4a, C-9a, C-10
4a	135.7, C			132.3, C		
5	108.7, CH	7.13 (d, 2.34)	C-6, C-8a, C-10, C-10a	108.9, CH	7.06 (d, 2.2)	C-6, C-8a, C-10, C-10a
6	165.5, C			165.1, C		
7	109.1, CH	6.60 (d, 2.4)	C-5, C-6, C-8, C-8a	108.2, CH	6.54 (d, 2.2)	C-5, C-6, C-8, C-8a
8	164.5, C			164.3, C		
8a	108.3, C			108.7, C		
9	189.4, C			189.2, C		
9a	111.1, C			108.4, C		
10	181.2, C			181.4, C		
10a	135.1, C			135.1, C		
1′	113.5, CH	6.54 (d, 5.7)	C-3, C-2', C-3', C-4'	62.9, CH ₂	3.72 (m)	C-2, C-2', C-3'
2′	43.7, CH	4.16 (t, 7.0)	C-1, C-2, C-3, C-3', C-4'	35.4, CH	3.48 (m)	C-1', C-4'
3′	67.4, CH ₂	4.10 (t, 8.2); 3.50 (m)	C-1', C-2'	32.7, CH ₂	1.92 (m)	C-2, C-1', C-2', C-4'
4'	30.4, CH ₂	2.18 (m)	C-2, C-1', C-2', C-3'	60.2, CH ₂	3.30 (m)	C-2', C-3'
1-OH					12.7 (s)	
3-OH					11.1 (s)	
6-OH					12.1 (s)	
8-OH					11.2 (s)	

Abbreviations: DMSO, dimethylsulfoxide; HMBC, heteronuclear multiple bond correlation.

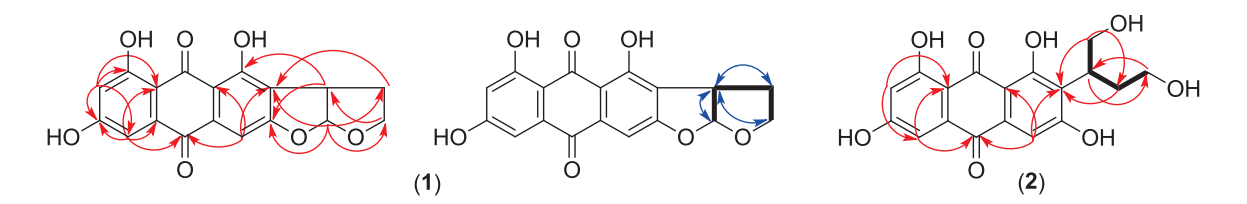


FIGURE 2 HMBC (red arrows), ¹H-¹H COSY (bold bonds), and NOESY (blue arrows) correlations observed for versicolorin C (1) and versiconol (2)

confirm that the 1,2,3,4,5-substituted benzene moiety was also fused to the quinone moiety.

The ¹H-¹H COSY data indicated an additional CH₂-CH₂-CH-CH spin system, constituted of resonances at δ_H 4.10/3.50 (δ_C 67.4, CH₂-3'), δ_{H} 2.18 (m; δ_{C} 30.4, CH₂-4'), δ_{H} 4.16 (t, J = 7.0 Hz; $\delta_{\rm C}$ 43.7, CH-2'), and $\delta_{\rm H}$ 6.54 (d, J = 5.7 Hz; $\delta_{\rm C}$ 113.5 CH-1'). The presence of two fused tetrahydrofuran rings was confirmed by

analysis of the HMBC spectrum, which showed correlations from H-1' to C-2', C-3', and C-4', as well as from H-2' to C-3' and C-4', between H-3', C-1' and C-2', as well as between H-4', C-1', C-2', and C-3'. The HMBC cross-peaks observed between H-1' and C-3, between H-2', C-1, C-2 and C-3, and between H-4' and C-2 enabled the connection of the two-furan ring to the 1,2,3,4,5substituted benzene moiety.

15214184, 2022. 4, Downloaded from https://onlinelibrary.wiley.com/doi/10.1002/ardp.202100441 by Univ of Sao Paulo - Brazil, Wiley Online Library on [16/05/2024]. See the Terms

ditions) on Wiley Online Library for rules of use; OA articles are governed by the applicable Creative Common:

Coupling constants observed between H-1' and H-2' (J = 5.7 Hz) and the NOESY correlations (see the Supporting Information) of the hydrogens at the fusion of the two tetrahydrofuran moieties of 1 revealed a *cis* ring junction at C-1' and C-2' (S^* , R^*). [17-20] These data confirmed the planar structure of versicolorin C (1).

Versiconol (2) was isolated as an orange amorphous powder. It showed an [M–H]⁻ ion in its HRESITOF mass spectrum at m/z 359.0804, corresponding to the formula $C_{18}H_{16}O_8$, with 11 Dl. The 1H and ^{13}C NMR spectra of $\bf 2$ were very similar to those of $\bf 1$, except for the signals of the two fused tetrahydrofuran rings in $\bf 1$ that were replaced by signals of a CH_2 –CH– CH_2 – CH_2 spin system (Table 1) in $\bf 2$. Analysis of the 1H – 1H COSY spectrum clearly indicated sequential couplings from δ_H 3.72 (m; δ_C 62.9, CH_2 - 1) through δ_H 3.48 (m; δ_C 35.4, CH- 2) and δ_H 1.92 (m; δ_C 32.7, CH_2 - 3) to δ_H 3.30 (m; δ_C 60.2 CH_2 - 4). This substructure was confirmed by analysis of the HMBC spectrum. The HMBC cross-peaks observed between H-1' and H-3' with C-2 enabled the connection of the system CH_2 –CH– CH_2 – CH_2 to the 1,2,3,4,5-substituted benzene moiety.

Comparison of UV and NMR data of **2** with that of versiconol^[18–25] allowed us to unambiguously establish its structure.

Following the structural elucidation of compounds 1 and 2, comparisons of experimental and simulated ECD data using density functional theory (DFT) were carried out to determine the absolute configuration of both anthraquinones. The experimental

spectra were recorded in MeOH solutions. Calculations were performed at the CAM-B3LYP/PCM(MeOH)/TZVP//B3LYP/PCM (MeOH)/6-31G(d) level for both compounds. Since the configuration at the ring fusion of compound 1 was established as cis by NMR analysis, calculations were carried out only for the 1'S2'R configuration. The spectrum of its enantiomer was obtained simply by multiplying the ECD spectrum calculated for 1'S2'R by (-1). The excellent agreement between observed and simulated UV/ECD data (Figures 3 and 4) led to the assignment of compound (-)-1 as 1'R,2'S and compound (-)-2 as 2'S. It is noteworthy that the lowest-energy conformers identified for compound 2 (Figure 4) revealed an extended intramolecular hydrogen-bond network, predicted to persist even in MeOH solution. Multiple chelated hydroxyl groups were in fact observed in the ¹H NMR spectra recorded in dimethylsulfoxide (DMSO) solution; however, no hydrogen-bonding information was available in MeOH due to solubility issues. Therefore, VCD experiments and calculations were performed to independently confirm the absolute configuration assigned to 2 by ECD. Infrared (IR) and VCD spectra recorded in DMSO were compared to DFT-simulated data at the B3PW91/ PCM(DMSO)/6-31G(d,p) level. The best agreement between observed and calculated data was obtained considering one explicit DMSO molecule in the calculations. IR and VCD spectra analysis confirmed the absolute configuration of (-)-2 as 2'S (Figure S18).

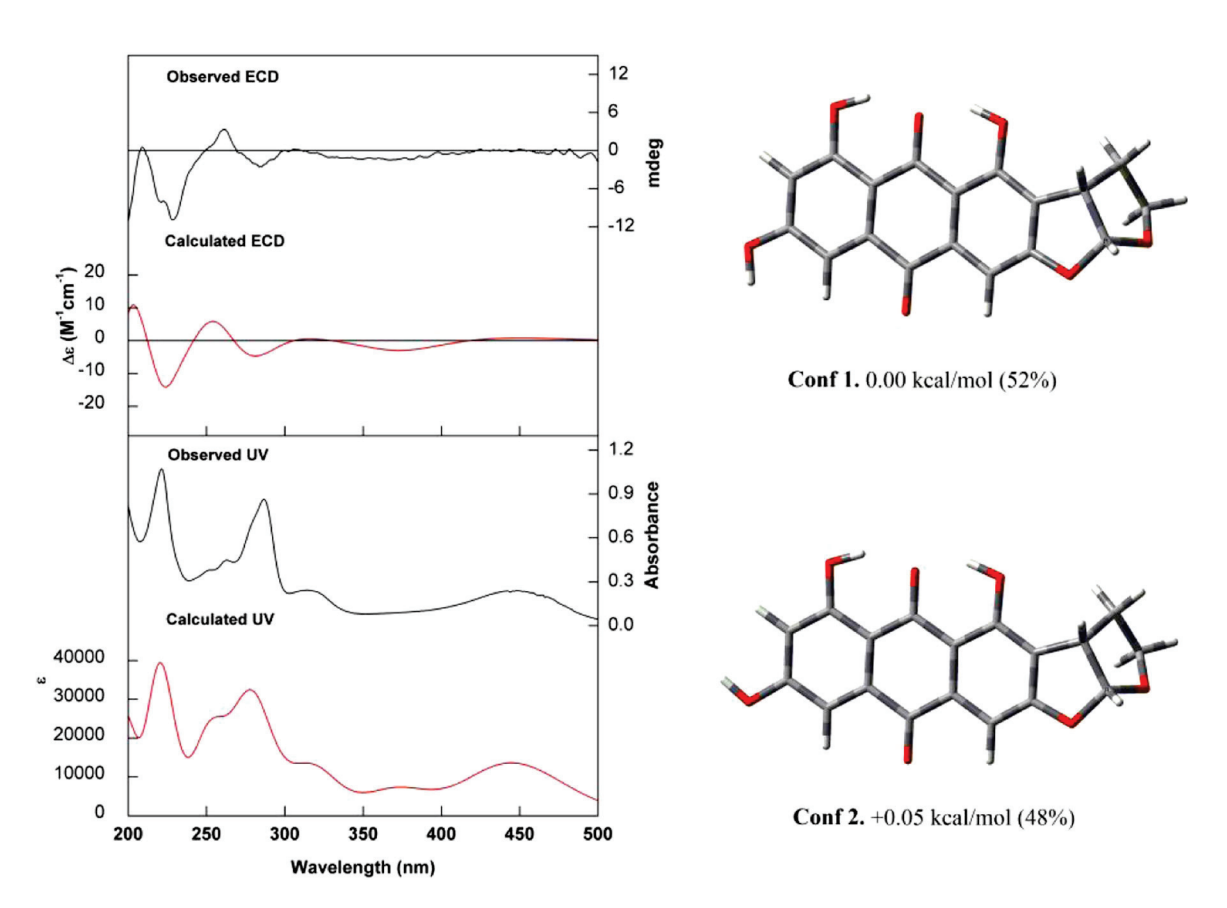


FIGURE 3 (Left) Comparison of experimental UV and electronic circular dichroism (ECD) spectra of (–)-1 in MeOH (black) with calculated (CAM-B3LYP/PCM(MeOH)/TZVP, red) spectra for (1'R,2'S)-1. (Right) Optimized structures, relative energies, and Boltzmann populations of the lowest-energy conformers identified for (1'R,2'S)-1 at the B3LYP/PCM(MeOH)/6-31G(d) level

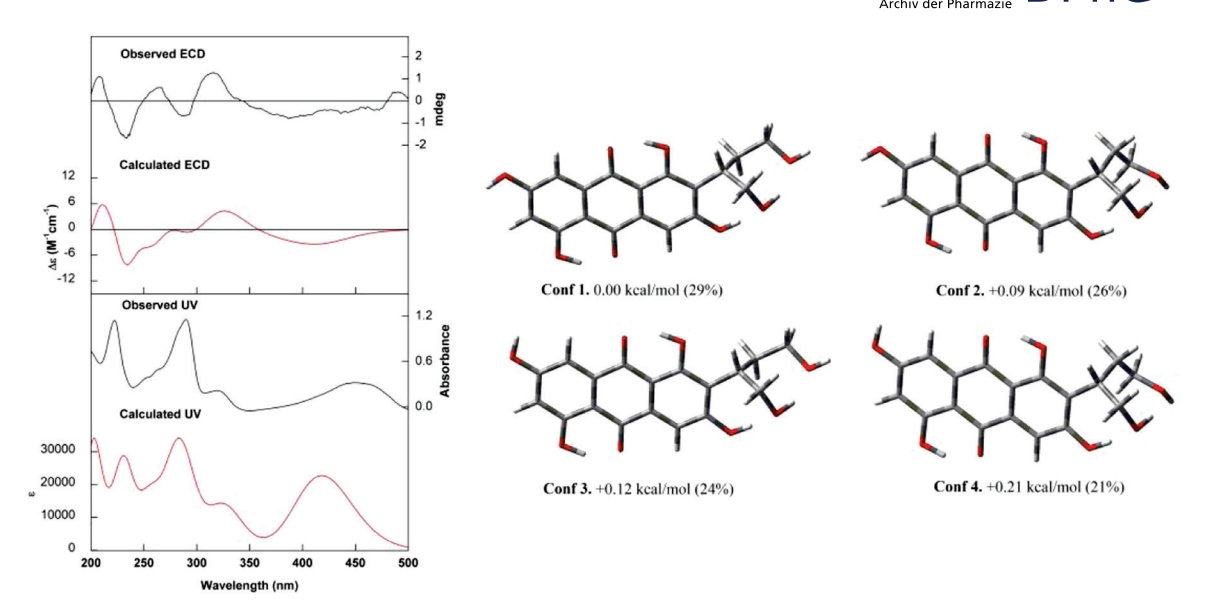


FIGURE 4 (Left) Comparison of experimental UV and electronic circular dichroism (ECD) spectra of (-)-2 in MeOH (black) with calculated (CAM-B3LYP/PCM(MeOH)/TZVP, red) spectra for (2'S)-2. (Right) Optimized structures, relative energies, and Boltzmann populations of the lowest-energy conformers identified for (2'S)-2 at the B3LYP/PCM(MeOH)/6-31G(d) level

2.2 | Pharmacology/biology

2.2.1 | In vitro anticancer activity

Compounds **1** and **2** were tested for their in vitro antiproliferative activity against human ovarian cancer cells OVCAR3, with IC $_{50}$ values of 0.24 μ M for **1** and of 1.07 μ M for **2**, while the IC $_{50}$ value for taxol (paclitaxel, control) was 7 ± 2 nM. Both compounds **1** and **2** were also tested for in vitro antibacterial and antifungal activity, against *Bacillus subtilis*, *Escherichia coli* BW25113, *E. coli* ATCC 10536, *Staphylococcus aureus* ATCC 25923, *Rhizoctonia solani* CMAA 1589, and *Colletotrichum falcatum*, but no activity was observed for **1** and **2**.

Versicolorin C (1) and versiconol (2) are related to aflatoxin biosynthesis in *Aspergillus* species. [17-28] Both 1 and 2 have been previously isolated from cultures of *Aspergillus versicolor*, *Aspergillus parasiticus*, *Aspergillus* sp. F40, *Aspergillus ustus*, and *Aspergillus nidulans*. [17-28] Versiconol showed weak antibacterial activity against *S. aureus* ATCC 25923 and *Vibrio parahaemolyticus* ATCC 17802. They also inhibited epidermal growth factor receptor protein tyrosine kinase and presented weak cytotoxicity activity against five human tumor cell lines. [21-28] Versicolorin C was found to be a potent activator of pancreatic deoxyribonuclease activity. [17-20]

3 | CONCLUSION

In summary, we reported for the first time the complete spectroscopic characterization, including the absolute configuration, of versicolorin C (1) and versiconol (2) isolated from cultures of *Aspergillus* sp. SDC28. Both compounds 1 and 2 showed significant cytotoxic activity against human ovarian cancer cells OVCAR3.

4 | EXPERIMENTAL

4.1 | Chemistry

4.1.1 | General

Optical rotations were recorded on a Polartronic H Schmidt+ Haensch polarimeter. UV spectra were obtained on a UV-3600 Shimazu UV spectrophotometer in MeOH at a concentration of 0.01 mg ml⁻¹. NMR spectra were obtained at 25°C, with tetramethylsilane as an internal standard, using a Bruker AV-600 spectrometer operating at either 600 MHz (¹H) or 150 MHz (¹³C) with a 2.5 mm cryoprobe. The acquisition of high-resolution mass spectra in the centroid MS mode was performed in positive and negative resolution modes, an acquisition time of 0-10 min, an ESI source, a mass range of 100-1200 Da, and a scan time of $0.2 \,\mathrm{s}^{-1}$. The positive and negative mode ESI conditions were as follows: 1.2 kV capillary voltage, 30 V cone voltage, 100°C source temperature, desolvation temperature of 450°C, 50 L h⁻¹ cone gas flow, and 750 L h⁻¹ desolvation gas flow. For internal calibration, a solution of leucine enkephalin (Sigma) 200 pg ml⁻¹ infused by the lock-mass probe at a flow rate of 10 μl min⁻¹ was used. UPLC-QToF-MS analyses were performed using a BEH C_{18} column (dimensions: 2.1×100 mm, $1.7 \, \mu m$; Waters Corporation) and a mobile phase consisting of Milli-Q + 0.1% formic acid (Panreac) and MeCN (Sigma) + 0.1% formic acid. The elution gradient used was from 90:10 of H₂O/MeCN to 100 MeCN for 7 min, maintained in 100% of MeCN for 2 min and H₂O/MeCN 90:10 for 0.9 min, flow rate of 0.50 ml min⁻¹. The column was maintained at a temperature of 40°C, and the samples were maintained at 15°C. Samples were diluted in MeOH at a concentration of 0.01 mg ml⁻¹. HPLC-UV-MS analyses were carried out on a Waters

of use; OA articles are governed by the applicable Creative Commons

5214184, 2022, 4, Downloaded from https://onlinelibrary.wiley.com/doi/10.1002/ardp.202100441 by Univ of Sao Paulo - Brazil, Wiley Online Library on [16/05/2024]. See the Terms

chromatography system consisting of a Waters 2695 Alliance control system coupled to a Waters 2696 UV-visible spectrophotometric detector with a photodiode array detector, connected sequentially to a Waters Micromass ZQ 2000 mass spectrometry detector operated using the Empower platform. Analyses were performed using a Waters C₁₈ X-Terra reversed-phase column (4.6 × 250 mm, 5 mm). The mass spectrometer detector was optimized using the following conditions: capillary voltage: 3 kV; temperature of the source: 100°C; desolvation temperature: 350°C; ESI mode, acquisition range 150–1200 Da; gas flow without a cone: $50 L h^{-1}$; and desolvation gas flow: 350 L h⁻¹. Samples were diluted in MeOH at a concentration of 2 mg ml^{-1} . The UV and ECD spectra of $\mathbf{1}$ and $\mathbf{2}$ were recorded using a Jasco J-810 spectrometer in the 200-500 nm region using the following parameters: three accumulations; room temperature; sample in methanol solution; 0.1 cm cell path length; and a concentration of 0.3 mg ml⁻¹. IR and VCD spectra were measured using a ChiralIR-2X FT-VCD spectrometer (BioTools Inc.) using a resolution of 4 cm⁻¹ and a collection time of 20 h. The optimum retardation of the ZnSe photoelastic modulator was set at 1400 cm⁻¹. Minor instrumental baseline offsets were eliminated from the final spectra by subtracting the VCD spectra of compound 2 from that obtained for the solvent, under the same conditions. The IR and VCD spectra were recorded in a BaF_2 cell with 100 μm path length using DMSO- d_6 as a solvent. The sample was prepared by dissolving 4.0 mg of compound 2 in 130 μl of solvent.

4.1.2 | General procedure for the *Aspergillus* sp. (SDC28) strain isolation and identification

The fungus Aspergillus sp. SDC28 was isolated from sediment samples collected in the twilight zone inside the Catão cave, located in the São Desidério karst area, state of Bahia, Brazil.[1,2] The fungus was isolated and identified by Paula et al.[1] at the genus level, even using two genetic markers for identification (β -tubulin). The phylogenetic tree analysis suggested that this fungus probably belongs to a new species. The fungus is maintained in the collection of the Departamento de Ecologia e Biologia Evolutiva of São Carlos Federal (UFSCar, São Carlos, SP, Brazil) and deposited at the Brazilian Collection of Environmental and Industrial Microorganisms under the accession number CBMAI 1926. The β -tubulin sequence used to identify the strain was deposited in GenBank (MF134413).

4.1.3 | General procedure for the extraction and isolation of compounds

Aspergillus sp. SDC28 strain was grown in 2% malt extract broth medium. Twenty-nine liters of malt extract broth was incubated under static conditions. After 33 days, fungal cultures were blended with EtOAc. The mixture of the growth medium and EtOAc was sonicated in an ultrasound bath for 10 min and then filtered through

a celite pad. The organic fraction was separated by decantation after liquid-liquid partitioning. The EtOAc fraction was evaporated, dried, solubilized in H₂O/MeOH 5:95 (v/v), and subjected to partition with hexane three times. The MeOH soluble fraction was named SDC28M (10,448.6 g). The SDC28M was subjected to open dry column chromatography with a cyanopropyl-bonded silica gel (10 g) eluted with 1 L of 1:1 hexane/CH₂Cl₂, 100% CH₂Cl₂, 1:1 CH₂Cl₂/EtOAc, 100% EtOAc, 1:1 EtOAc/MeOH, and 100% MeOH. The collected fractions were concentrated to dryness to afford fractions named SDC28M1 (5,884.4 mg), SDC28M2 (2,005.8 mg), SDC28M3 (986.5 mg), SDC28M4 (121.7 mg), SDC28M5 (1,253.9 mg), and SDC28M6 (135.8 mg).

Fractions SDC28M3, SDC28M4, and SDC28M5 were combined and separated by size exclusion chromatography on a Sephadex LH- 20^{\circledR} column and eluted with MeOH, resulting in 350 fractions of 10 ml each. Fractions were combined in 34 additional fractions after analysis by thin-layer chromatography using phosphomolybdic acid, followed by heating at 50°C for 5 min. Fluorescent substances were visualized under UV light (λ_{max} = 254 and 366 nm).

Fraction SDC28M35-23 (18.7 mg) was subjected to an HPLC separation using an analytical Inertsil® ODS-4 column (4.0 × 250 mm, 5 μ m) at a flow rate of 1.0 ml min $^{-1}$ for 45 min, with H₂O/MeOH 1:1 (v/v) as an eluent and detection at λ_{max} 254 and 280 nm. Three fractions were obtained (SDC28M35-23A to SDC28M35-23C). Fraction SDC28M35-23B was identified as versiconol (2, 3.9 mg).

Fraction SDC28M35-24 (36.3 mg) was subjected to an HPLC separation using an analytical Inertsil® ODS-4 column (4.0 × 250 mm, 5 µm) at a flow rate of 1.0 ml min $^{-1}$ for 35 min, with H $_2$ O/MeOH 1:1 (v/v)+0.1% trifluoroacetic acid (TFA) as an eluent and detection at $\lambda_{\rm max}$ 254 and 280 nm. Eight fractions were obtained (SDC28M35-24A to SDC28M35-24H). Fractions SDC28M35-24F and SDC28M35-24G were identified as versiconol (2, 15.8 mg).

Fractions SDC28M35-25 (18.8 mg), SDC28M35-26 (7.5 mg), and SDC28M35-27 (17.4 mg) were combined (SDC28M35-257) and purified by HPLC using an InertSustain® C₁₈ analytical column $(4.6 \times 250 \, \text{mm}, \, 5 \, \mu \text{m})$ with $40:60 \, H_2 \text{O/MeOH} + 0.1\%$ TFA as the eluent at a flow rate of 1.0 ml min⁻¹ for 80 min, and the eluate was monitored at λ_{max} 254 and 280 nm. Eight fractions were obtained (SDC28M35-257A to SDC28M35-257H). Fractions SDC28M35-257E (3.5 mg) and SDC28M35-257F (3.9 mg) were combined (SDC28M35-257EF) and purified by HPLC using an Inertsil® ODS-4 analytical column ($4.0 \times 250 \,\text{mm}$, $5 \,\mu\text{m}$) with $30:70 \,\text{H}_2\text{O}/\text{MeOH} +$ 0.1% TFA as the eluent at a flow rate of 1.0 ml min⁻¹ for 30 min, and the eluate was monitored at λ_{max} 254 and 280 nm. Five fractions were obtained (SDC28M35-257EF1 to SDC28M35-257EF5). Fraction SDC28M35-257EF2 was identified as versiconol (2, 4.4 mg). Fractions SDC28M35-257EF4 (1.1 mg) and SDC28M35-257EF5 (0.5 mg) were identified as versicolorin C (1, 1.6 mg).

Fractions SDC28M35-28 (6.3 mg) and SDC28M35-29 (23.2 mg) were combined (SDC28M35-289) and subjected to HPLC separation using an InertSustain $^{\oplus}$ C₁₈ analytical column (4.6 × 250 mm, 5 µm) with 45:55 H₂O/MeOH as the eluent at a flow rate of 1.0 ml min $^{-1}$ for 40 min, and the eluate was monitored at λ_{max} 220 and 254 nm.

Four fractions were obtained (SDC28M35-289A to SDC28M35-289D). Fraction SDC28M35-289B was identified as versicolorin C (1, 1.6 mg).

Fractions SDC28M35-30 (7.8 mg), SDC28M35-31 (22.5 mg), and SDC28M35-32 (5.8 mg) were pooled (SDC28M35-302) and subjected to HPLC separation using an InertSustain® C₁₈ analytical column $(4.6\times250\,\text{mm},\,5\,\mu\text{m})$ with 30:70 $\text{H}_2\text{O}/\text{MeOH}$ as the eluent at a flow rate of 1.0 ml min⁻¹ for 45 min, and the eluate was monitored at λ_{max} = 254 and 280 nm. Seven fractions were obtained (SDC28M35-302A to SDC28M35-302G). Fraction SDC28M35-302B (9.4 mg) was separated by HPLC using an Inertsil® ODS-4 analytical column $(4.0 \times 250 \text{ mm}, 5 \mu\text{m})$ with 1:1 H₂O/MeOH + 0.3% TFA as the eluent at a flow rate of 1.0 ml min⁻¹ for 40 min, and the eluate was monitored at λ_{max} = 254 and 280 nm. Seven fractions were obtained (SDC28M35-302B1 to SDC28M35-302B7). Fractions SDC28M35-302B3 (1.8 mg) and SDC28M35-302B4 (2.0 mg) were identified as versiconol (2, 3.8 mg). Fractions SDC28M35-302F (3.7 mg) and SDC28M35-302G (0.6 mg) were combined (SDC28M35-302FG) and purified by HPLC using an Inertsil® ODS-4 analytical column (4.0 × 250 mm, 5 μm) with 30:70 $H_2O/MeOH + 0.3\%$ TFA as the eluent at a flow rate of 1.0 ml min^{-1} for 35 min, and the eluate was monitored at λ_{max} = 254 and 280 nm. Seven fractions were obtained (SDC28M35-302FG1 to SDC28M35-302FG7). Fractions SDC28M35-302FG5 and SDC28M35-302FG7 were identified as versicolorin C (1, 1.8 mg). The final production titers were 6.2×10^{-5} and 1.3×10^{-4} g/L for compounds 1 and 2, respectively.

Versicolorin C (1)

Orange amorphous powder; [α] $_{0}^{25}$ –123.5 (c 0.20, MeOH). UV (MeOH) λ_{max} nm (log ϵ) 222 (6.24), 289 (6.36), 319 (6.40), 451 (6.55). 1 H (600 MHz, DMSO- d_{6}) and 13 C NMR (150 MHz, DMSO- d_{6}) data were found to be consistent with those reported in the literature. $^{[17-19]}$ HRESITOFMS m/z 339.0506 [M-H] $^{-}$ (calcd for $C_{18}H_{12}O_{7}$, 339.0505).

Versiconol (2)

Orange amorphous powder; [α] $_{0}^{25}$ –113.0 (c 0.20, MeOH). UV (MeOH) λ_{max} nm (log ϵ) 222 (6.09), 292 (6.21), 321 (6.25), 458 (6.40). 1 H (600 MHz, DMSO- d_{6}) and 13 C NMR (150 MHz, DMSO- d_{6}) spectroscopic data were found to be consistent with those reported in the literature. $^{[20-22]}$ HRESITOFMS m/z 361.0933 [M+H] $^{+}$ and 359.0804 [M-H] $^{-}$ (calcd for $C_{18}H_{16}O_{8}$, 361.0923, and 359.0767).

4.1.4 | General procedure for the calculations

All DFT and time-dependent DFT (TDDFT) calculations were carried out at 298 K in MeOH solution using the polarizable continuum model (PCM) in its integral equation formalism version (IEFPCM) incorporated in Gaussian 09 software. [29] Calculations were performed for the arbitrarily chosen (1'S,2'R)-1 and (2'S)-2. Conformational searches were carried out at the molecular mechanics level of theory using the MMFF force field incorporated in the Spartan 08 software package. Initially, five conformers of (1'S,2'R)-1 and 100 conformers

of (2'S)-2, with a relative energy (rel E.) within 10 kcal mol⁻¹ of the lowest-energy conformer, were selected and further geometry was optimized at the B3LYP/PCM(MeOH)/6-31G(d) level. The two conformers of (1'S,2'R)-1 with rel E. < 2.2 kcal mol⁻¹, and the four conformers of (2'S)-2 with rel E. < 1.7 kcal mol⁻¹ were selected for UV and ECD spectral calculations. Vibrational analysis resulted in no imaginary frequencies for all conformers, confirming them as real minima. TDDFT was used to calculate the excitation energy (in nm) and rotatory strength R in the dipole velocity (R_{vel} in cgs units: $10^{-40}\,\text{esu}^2\,\text{cm}^2)$ form, at the CAM-B3LYP/PCM(MeOH)/TZVP level. The calculated rotatory strengths from the first 30 singlet → singlet electronic transitions were simulated into an ECD curve using Gaussian bands with a bandwidth of σ 0.25 eV. The predicted wavelength transitions were multiplied with a scaling factor of 1.1, determined by the best agreement between the experimental and calculated UV spectra. The Boltzmann factor for each conformer was calculated based on Gibbs free energies. The ECD spectrum of (1'R,2'S)-1 presented in Figure 3 was obtained by multiplying the spectrum calculated for (1'S,2'R)-1 by -1. The same four conformers identified at the B3LYP/PCM(MeOH)/6-31G(d) level were reoptimized and their IR/VCD data were calculated at the B3PW91/ PCM(DMSO)/6-31G(d,p) level. Following initial comparisons of experimental and calculated data, further calculations were carried out with explicit DMSO molecules hydrogen-bonded to different hydroxyl groups. The best agreement of experiment and simulation was found for the hydrogen bond between a single DMSO molecule and the hydroxyl group at C-6. IR and VCD spectra were created using dipole and rotational strengths from Gaussian, which were calculated at the same level as that used during the geometry optimization step and converted into molar absorptivities (M⁻¹ cm⁻¹). Each spectrum was plotted as a sum of Lorentzian bands with half-widths at a halfmaximum of 6 cm⁻¹. The calculated wavenumbers were multiplied by a scaling factor of 0.97. The final spectra were generated using a simple average of the lowest-energy conformers identified for 2 and plotted using Origin 8 software.

4.2 | Pharmacological/biological assays

4.2.1 | Cytotoxicity assays

Human ovarian cancer cells OVCAR3 were purchased from the American Type Culture Collection (Manassas, VA). The cell line was propagated at 37°C in 5% CO $_2$ in RPMI 1640 medium, supplemented with fetal bovine serum (10%), penicillin (100 U ml $^{-1}$), and streptomycin (100 $\mu g \, \text{ml}^{-1}$). Cells in log-phase growth were harvested by trypsinization, followed by two washing steps to remove all traces of enzyme. A total of 5000 cells were seeded per well of a 96-well clear, flat-bottom plate (Microtest 96 $^{\$}$, Falcon) and incubated overnight (37°C in 5% CO $_2$). Samples dissolved in DMSO were then diluted and added to the appropriate wells. The cells were incubated in the presence of the test substance for 72 h at 37°C and evaluated for viability using a commercial absorbance assay (CellTiter-Blue $^{\$}$ Cell Viability Assay, Promega Corp.) that measured

viable cells. IC_{50} values are expressed in μM relative to the solvent (DMSO) control. Measurements were recorded on a BioTek plate reader measuring absorbance at 600 nm. Positive controls are included on screening plates (taxol at 10 nM). Human ovarian cancer cells OVCAR3 are STR validated annually.

ACKNOWLEDGMENTS

The authors thank Dr. Fernanda R. da Costa and Dr. Andrea D. S. Silva (LNBio-CNPEM) for performing the antibacterial assays. Financial support was provided by the São Paulo State Research Foundation (FAPESP), Brazil (BIOTA/BIOprospecTA FAPESP grant 2013/50228-8 and SPEC grant 2017/12436-9 to R. G. S. B., regular grant 2019/22319-5 to J. M. B., postdoctoral scholarship 2017/06014-4 to J. R. G., and PhD scholarship 2016/21341-9 to D. I. B.), and by NIH (P01CA125066) to J. E. B. The authors thank Coordenação de Aperfeiçoamento de Pessoal de Nível Superior—Brazil (CAPES)—Finance Code 001. This study was also supported by resources supplied by the Centre for Scientific Computing (NCC/GridUNESP) of São Paulo State University (UNESP).

CONFLICT OF INTERESTS

The authors declare that there are no conflicts of interests.

ORCID

João M. Batista http://orcid.org/0000-0002-0267-2631

Roberto G. S. Berlinck http://orcid.org/0000-0003-0118-2523

REFERENCES

- C. C. P. Paula, Q. V. Montoya, L. A. Meirelles, C. F. Sanchez, A. Rodrigues, M. H. R. Seleghim, An. Acad. Bras. Cienc. 2019, 91(3), e20180583. https://doi.org/10.1590/0001-3765201920180583
- [2] C. C. P. Paula, Q. V. Montoya, A. Rodrigues, M.E. Bichuette, M. H. R. Seleghim, J. Cave Karst Stud. 2016, 78(3), 208.
- [3] D. E. Northup, K. H. Lavoie, Geomicrobiol. J. 2001, 18, 199.
- [4] E. L. S. Taylor, M. A. A. R. Stoianoff, R. L. Ferreira, Int. J. Speleol. 2013, 42(3), 267.
- [5] A. Nováková, Int. J. Speleol. 2009, 38(1), 71.
- [6] Z. F. Zhang, P. Zhao, L. Cai, Front. Microbiol. 2018, 9, 1407.
- [7] K. J. Vanderwolf, D. Malloch, D. F. McAlpine, G. J. Forbes, Int. J. Speleol. 2013, 42(1), 77.
- [8] V. Jurado, L. Laiz, V. Rodriguez-Nava, P. Boiron, B. Hermosin, S. Sanchez-Moral, C. Saiz-Jimenez, Int. J. Speleol. 2010, 39(1), 15.
- [9] L. Belyagoubi, N. Belyagoubi-Benhammou, V. Jurado, J. Dupont, S. Lacoste, F. Djebbah, F. Z. Ounadjela, S. Benaissa, H. Salim, D. E. Abdelouahid, C. Saiz-Jimenez, *Int. J. Speleol.* 2018, 47(2), 189.
- [10] E. L. S. Taylor, G. F. Ferreira, G. J. C. De Freitas, R. L. Ferreira, D. A. Santos, M. A. Resende-Stoianoff, Int. J. Speleol. 2017, 46(3), 369.
- [11] D. G. Tavares, B. V. L. Barbosa, R. L. Ferreira, W. F. Duarte, P. G. Cardoso, *Biocatal. Agric. Biotechnol.* 2018, 16, 148.
- [12] P. N. Costa Souza, D. G. Tavares, C. R. F. Souza, M. L. L. Martinez, W. P. Oliveira, L. H. S. Guimarães, P. G. Cardoso, *Braz. Arch. Biol. Technol.* 2020, 63, 1.
- [13] V. K. Gupta, New and Future Developments in Microbial Biotechnology and Bioengineering—Aspergillus System Properties and Applications. Elsevier. Amsterdam 2016.

- [14] M. Subhan, R. Faryal, I. Macreadie, J. Fungi 2016, 2, 13. https://doi. org/10.3390/jof2020013
- [15] W.-F. Xu, R. Chao, Y. Hai, Y.-Y. Guo, M.-Y. Wei, C.-Y. Wang, C.-L. Shao, J. Nat. Prod. 2021, 84(4), 1353.
- [16] W. Li, L. Ding, N. Wang, J. Xu, W. Zhang, B. Zhang, S. He, B. Wu, H. Jin, Mar. Drugs 2019, 17(5), 283. https://doi.org/10.3390/md17050283
- [17] K. Fukuyama, T. Tsukihara, Y. Katsube, T. Hamasaki, Y. Hatsuda, Bull. Chem. Soc. Jpn. 1975, 48(10), 2648.
- [18] J. C. Schabort, H. A. Roberts, Biochem. Pharmacol. 1971, 20(1), 243.
- [19] W. T. Shier, Y. Lao, T. W. J. Steele, H. K. Abbas, *Bioorg. Chem.* 2005, 33, 426.
- [20] A. G. Kozlovskii, T. V. Antipova, V. P. Zhelifonova, B. P. Baskunov, N. E. Ivanushkina, G. A. Kochkina, S. M. Ozerskaya, *Microbiology* 2017, 86(2), 176.
- [21] P. S. Steyn, R. Vleggaar, P. L. Wessels, R. J. Cole, D. B. Scott, J. Chem. Soc., Perkin Trans. 1 1979, 451.
- [22] F. Petersen, A. Dredenhagen, H. Mett, N. B. Lydon, R. Delmendo, H.-B. Jenny, H. H. Peter, J. Antibiot. 1995, 48(3), 191.
- [23] Y. M. Lee, H. Li, J. Hong, H. Y. Cho, K. S. Bae, M. A. Kim, D.-K. Kim, J. H. Jung, Arch. Pharmacal Res. 2010, 33(2), 231.
- [24] Y.-Q. Tian, S.-T. Lin, K. Kumaravel, H. Zhou, S.-Y. Wang, Y.-H. Liu, Phytochem. Lett. 2018. 27, 74.
- [25] P. S. Steyn, R. Vleggaar, P. L. Wessels, D. B. Scott, J. Chem. Soc., Perkin Trans. 1. 1979, 460.
- [26] K. Yabe, Y. Ando, T. Hamasaki, Microbiology 1991, 137(10), 2469.
- [27] M. F. Grau, R. Entwistle, C. E. Oakley, C. C. Wang, B. R. Oakley, ACS Chem. Biol. 2019, 14(7), 1643.
- [28] Y. Hatsuda, T. Hamasaki, M. Ishida, S. Yoshikawa, Agric. Biol. Chem. 1969, 33(1), 131.
- [29] M. J. Frisch, G. W. Trucks, H. B. Schlegel, G. E. Scuseria, M. A. Robb, J. R. Cheeseman, G. Scalmani, V. Barone, B. Mennucci, G. A. Petersson, H. Nakatsuji, M. Caricato, X. Li, H. P. Hratchian, A. F. Izmaylov, J. Bloino, G. Zheng, J. L. Sonnenberg, M. Hada, M. Ehara, K. Toyota, R. Fukuda, J. Hasegawa, M. Ishida, T. Nakajima, Y. Honda, O. Kitao, H. Nakai, T. Vreven, J. A. Montgomery, J. E. Peralta, F. Ogliaro, M. Bearpark, J. J. Heyd, E. Brothers, K. N. Kudin, V. N. Staroverov, R. Kobayashi, J. Normand, K. Raghavachari, A. Rendell, J. C. Burant, S. S. Iyengar, J. Tomasi, M. Cossi, N. Rega, N. J. Millam, M. Klene, J. E. Knox, J. B. Cross, V. Bakken, C. Adamo, J. Jaramillo, R. Gomperts, R. E. Stratmann, O. Yazyev, A. J. Austin, R. Cammi, C. Pomelli, J. W. Ochterski, R. L. Martin, K. Morokuma, V. G. Zakrzewski, G. A. Voth, P. Salvador, J. J. Dannenberg, S. Dapprich, A. D. Daniels, Ö. Farkas, J. B. Foresman, J. V. Ortiz, J. Cioslowski, D. J. Fox, Gaussian 09, Revision A.02, Gaussian, Wallingford, CT 2009.

SUPPORTING INFORMATION

Additional supporting information may be found in the online version of the article at the publisher's website.

How to cite this article: J. R. Gubiani, D. I. Bernardi, C. C. P. De Paula, M. H. R. Seleghim, A. G. Ferreira, A. N. L. Batista, jr., J. M. Batista, L. F. P. Oliveira, S. P. Lira, J. E. Burdette, R. G. S. Berlinck, *Arch. Pharm.* **2022**;355:e2100441.

https://doi.org/10.1002/ardp.202100441